

# An Investigation into the Role of Dislocation Climb during Intermediate Temperature Flow of Mg Alloys

Michael A. Ritzo,<sup>1</sup> Jishnu J. Bhattacharyya,<sup>1</sup> Ricardo A. Lebensohn,<sup>2</sup> and Sean R. Agnew<sup>1,\*</sup>

<sup>1</sup>Department of Materials Science and Engineering, University of Virginia,  
Charlottesville, VA 22904, USA

<sup>2</sup>Materials Science and Technology Division, Los Alamos National Laboratory, MS G755,  
Los Alamos, NM 87545, USA

## Abstract

Textured Mg alloy sheet samples were tensile tested parallel to the transverse direction, at Zener-Holloman parameter values ranging from  $Z \sim 50$  at room temperature and  $10^{-3} \text{ s}^{-1}$  down to  $Z \sim 18$  at  $350^\circ\text{C}$  and  $10^{-5} \text{ s}^{-1}$ . At high  $Z$ , the samples exhibit strong texture evolution indicative of significant prismatic slip of dislocations with  $\langle a \rangle$  Burgers vectors. Correspondingly, the plastic anisotropy is high,  $r \sim 4$ . At low  $Z$ , the texture evolution is minimal and the response is nearly isotropic,  $r \sim 1$ . Previously, it has been asserted that the high ductility and low plastic anisotropy observed at low  $Z$  conditions is due to enhanced activity of non-basal slip modes, including prismatic slip of  $\langle a \rangle$  dislocations and pyramidal slip of  $\langle a \rangle$  and  $\langle c+a \rangle$  dislocations. The present results call this understanding into question and suggest that the enhanced ductility is more closely associated with the climb  $\langle a \rangle$  dislocations.

## Keywords

texture, anisotropy, dislocation, climb, glide

## Introduction

The use of polycrystal plasticity modeling has radically changed our understanding of the deformation of hexagonal close packed (hcp) Mg alloys. Historically, it was believed that non-basal slip was not a significant contributor to the deformation of polycrystalline Mg alloys, unless the temperature was in excess of  $200^\circ\text{C}$  [e.g., 1]. Since that time, it has been repeatedly shown that non-basal slip of  $\langle a \rangle$  dislocations is surprisingly active in textured Mg alloy polycrystals, even at room temperature [e.g., 2]. Evidence in support of this fact are the observed high  $r$ -values of tensile tested Mg alloy sheets with strong basal textures, as well as the evolution of that texture toward one which exhibits near 6-fold symmetry in the prismatic pole figure. Along with this new understanding of the low temperature deformation came another surprising revelation. The relative activity of non-basal  $\langle a \rangle$  slip could not continue increasing at elevated temperatures because the  $r$ -values were shown to

---

\* [mar3dm@virginia.edu](mailto:mar3dm@virginia.edu), [jjb4cp@virginia.edu](mailto:jjb4cp@virginia.edu), [lebenso@lanl.gov](mailto:lebenso@lanl.gov), and corresponding author: [agnew@virginia.edu](mailto:agnew@virginia.edu)

decrease with temperature, not increase. Furthermore, the characteristic 6-fold feature in the prismatic pole figures becomes weaker, not stronger.

A possible solution to the problem was offered in terms of pyramidal  $\langle c+a \rangle$  slip, which provides the hcp crystals with a way to accommodate compression along their c-axes [e.g., 3]. It was shown that increasing the activity of  $\langle c+a \rangle$  slip would lead to a reduction in r-value (and even a reduction in the intensity of the 6-fold symmetric texture), in agreement with what is observed during higher temperature deformation. It was reasonably concluded that increased temperature must lead to increased activity of this thermally activated deformation mechanism. This hypothesis has become widely accepted, leading to a world-wide focus on better understanding the behavior of these unusual  $\langle c+a \rangle$  dislocations, which have a Burgers vector which is nearly twice as large as that of the common  $\langle a \rangle$ -type dislocation [e.g., 4,5,6]. Researchers have furthermore come to accept the notion that increasing  $\langle c+a \rangle$  slip activity may hold the key to unlocking potential ductility of Mg alloys [7,8,9]. The notion that  $\langle c+a \rangle$  slip occurs is not in question, because both texture data and TEM investigation have repeatedly shown evidence for this slip mode. However, the idea that increased temperature leads to greatly increased  $\langle c+a \rangle$  slip activity is not strongly supported by the data.

In this paper, we propose an alternative explanation for the changes in r-value and texture evolution, which are observed at elevated temperatures. *It is hypothesized that the climb of  $\langle a \rangle$  dislocations (rather than slip of non-basal dislocations) is responsible for the reduced r-values, altered texture evolution, and even improved ductility of textured Mg alloys which is observed at elevated temperatures.* The notion that dislocation climb becomes more important at elevated temperatures is not at all revolutionary. However, it has only recently become possible to explore the effect that dislocation climb will have on the anisotropy and texture evolution of textured polycrystals. Along with collaborators, one of the co-authors developed a viscoplastic self-consistent (VPSC) polycrystal modeling code, which accounts for the non-conservative (climb) motion of dislocations [10,11].

We begin by providing a brief introduction to the model, followed by a description of experimental methods and results which highlight the effects we are hoping to explain, and then enumerate simulation results which illustrate that a model which accounts for dislocation climb mediated flow can provide a satisfactory explanation for observed transitions in both anisotropy and texture evolution. Only tensile deformation of a well-studied case, basal textured Mg alloy AZ31B sheets is considered in this preliminary study. This avoids the complexity of simultaneous consideration of dislocation motion and deformation twinning-mediated plasticity. Only tensile deformation parallel to the sheet transverse direction is considered because previous studies have revealed this direction exhibits the most contrast with respect to the temperature-dependent phenomena of interest.

## Modeling background

Crystal plasticity models generally consider dislocation glide and twinning [12,13] as the only dissipative processes. In addition, both slip and twinning are assumed to be governed the generalized Schmid law, which computes the resolved shear stress on a slip system as follows:

$$\tau = \mathbf{m} : \boldsymbol{\sigma} \quad \text{Eq 1}$$

where  $\mathbf{m} = \text{sym}(\hat{\mathbf{b}} \otimes \hat{\mathbf{n}})$  is the Schmid tensor, which resolves the grain-level stress  $\boldsymbol{\sigma}$  onto the slip plane and in the slip direction [e.g., 14]. The role of cross-slip is usually loosely connected to the process of dynamic recovery [15], and dislocation climb is for the most part disregarded. Lebensohn et al. [10] generalized the connection between stress and dislocation motion, beyond the Schmid law of Eq. 1. by appealing to the full Peach-Koehler relationship,

$$\mathbf{f} = (\boldsymbol{\sigma} \cdot \mathbf{b}) \times \hat{\mathbf{t}} \quad \text{Eq 2}$$

where  $\mathbf{b}$  is the Burgers vector and  $\hat{\mathbf{t}}$  is the dislocation line direction. The forces which drive dislocation glide can then be parsed from those which drive climb. The force which drives glide is nothing other than the Schmid stress times the magnitude of the Burgers vector.

$$\mathbf{f}_g = \{(\boldsymbol{\sigma} \cdot \mathbf{b}) \times \hat{\mathbf{t}}\} \cdot \hat{\boldsymbol{\chi}} = \{\boldsymbol{\sigma} : (\hat{\mathbf{b}} \otimes \hat{\mathbf{n}})\} |\mathbf{b}| \quad \text{Eq 3}$$

where  $\hat{\boldsymbol{\chi}}$  is the direction of dislocation glide (orthogonal to the line direction). On the other hand, the climb force is resolved along the glide plane normal direction.

$$\mathbf{f}_c = \{(\boldsymbol{\sigma} \cdot \mathbf{b}) \times \hat{\mathbf{t}}\} \cdot \hat{\mathbf{n}} = -\{\boldsymbol{\sigma} : (\hat{\mathbf{b}} \otimes \hat{\boldsymbol{\chi}})\} |\mathbf{b}| \quad \text{Eq 4}$$

Notably, the glide force only depends upon the deviatoric stress (the addition of pressure has no effect), whereas the climb force depends on the full stress tensor. For dislocation glide, the dyadic cross product  $\hat{\mathbf{b}} \otimes \hat{\mathbf{n}}$  can be decomposed into symmetric (strain,  $\mathbf{m}$ ) and antisymmetric (rotation,  $\mathbf{q}$ ) components. Indeed, this slip-induced rotation is the basis of texture evolution during glide. For climb, the analogous tensor,  $\hat{\mathbf{b}} \otimes \hat{\boldsymbol{\chi}}$  can be decomposed into symmetric strain ( $\mathbf{k}$ ) and rotation ( $\mathbf{r}$ ) components. The distinct types of strain and rotation associated with climb and glide provide a means by which their contributions to the deformation may be parsed. For example, the strain rate within a crystal undergoing glide and climb may be expressed as a function the applied stress as follows.

$$\dot{\boldsymbol{\varepsilon}} = \sum_s \mathbf{m}^s \left( \frac{f^s}{\tau_c^s b^s} \right)^{n_g} \text{sign}(\mathbf{m} : \boldsymbol{\sigma}) + \sum_c \mathbf{k}^c \left( \frac{f^c}{\sigma_c b^c} \right)^{n_c} \text{sign}(\mathbf{k} : \boldsymbol{\sigma}) \quad \text{Eq 5}$$

Although it is not a focus of the present work, it is mentioned that the code incorporates an adaptation in which Lebensohn et al. [16] expanded the model to account for the “chemical” (or osmotic) force due to the non-equilibrium vacancy concentration that will develop in the vicinity of the climbing dislocations was expressed as follows:

$$\mathbf{f}_{chem} = \left\{ \frac{kT}{\Omega} \ln \left( \frac{c}{c_{0,PT}} \right) \mathbf{I} : (\hat{\mathbf{b}} \otimes \hat{\boldsymbol{\chi}}) \right\} |\mathbf{b}| \quad \text{Eq 6}$$

where  $k$  is Boltzman’s constant,  $\Omega$  is the atomic volume,  $c$  is the vacancy concentration near the dislocation, and  $c_{0,PT}$  is the equilibrium vacancy concentration at the given pressure and temperature, and  $\mathbf{I}$  is the identity matrix. The relationship is further complicated by the fact that one must track the character of dislocations in order to implement the climb model. Indeed the “climb strain tensor,”  $\mathbf{k} = \text{sym}(\hat{\mathbf{b}} \otimes \hat{\boldsymbol{\chi}})$ , can be expressed in terms of the angle between the Burgers vector and line direction.

In this study, the experimentally measured texture is used as an input and boundary conditions appropriate for uniaxial tension parallel to the sheet transverse direction (TD) are imposed. The parameters which were explored include the relative critical resolved shear strengths ( $\tau$ ) of the basal  $\langle a \rangle$ , prismatic  $\langle a \rangle$ , and pyramidal  $\langle c+a \rangle$  for a number of glide-only cases. Upon determining which cases were most relevant, we then explored the effect of incorporating climb of  $\langle a \rangle$  dislocations. The outputs presently under consideration are the  $r$ -value and the evolved texture after TD tension. The power law exponents employed in this study were fixed at  $n_g = 20$  and  $n_c = 3$ , though further exploration of the effects of these parameters on the constitutive response and texture evolution is merited.

## Experimental methods

Mg alloy AZ31B sheet with 1mm thickness was provided by the former Magnesium Elektron North America, part of the Luxfer group. The samples were examined in the O temper, which involves warm rolling followed by annealing at 340°C for 1 hr. The microstructure of the samples had been examined in previous study and found to be comprised of equiaxed grains with a lineal intercept grain size of  $\sim 8.3 \pm 0.1 \mu\text{m}$  with only occasional twins from the prior deformation [17]. The texture is

measured using X-ray diffraction from the sheet midplane, both before and after deformation, using a Panalytical X'pert Pro MPD diffractometer, as described previously [17]. The texture analysis and graphing were performed using the MTEX toolbox for MATLAB.

Tensile samples with a test geometry developed for examining the superplastic behavior of sheet metals [18] were cut from the sheets using electrodischarge machining. The effective gage section of the samples is approximately 38 mm long by 6 mm wide. The  $r$ -values were measured as the ratio of the logarithmic true plastic strains along the width and thickness directions, after deforming the samples to a plastic strain of 0.08 – 0.12 along the TD. One test of the accuracy of the strain measurements was to examine volumetric strain implied, and since plasticity is known to be volume constant, only those measurements with implied absolute dilatation of less than  $\sim 0.005$  were retained in the final analysis.

Tensile tests were performed at temperatures ranging from room temperature up to 350°C, at strain rates ranging from  $1\text{E-}5\text{ s}^{-1}$  up to  $1\text{E-}3\text{ s}^{-1}$ . The tensile test data were analyzed in terms of the flow stress measured at a plastic strain of 0.10. The test conditions were chosen in order to obtain a wide range of Zener-Holloman parameter,  $Z$ , also known as the temperature compensated strain rate:

$$Z = \dot{\epsilon} \exp\left(\frac{Q}{RT}\right) \quad \text{Eq 7}$$

where  $Q$  is the activation energy and  $R$  is the universal gas constant. Sellars & Tegart [19] suggested a hyperbolic sine function would describe the relationship between rate and flow stress over a wide range of hot working and creep conditions.

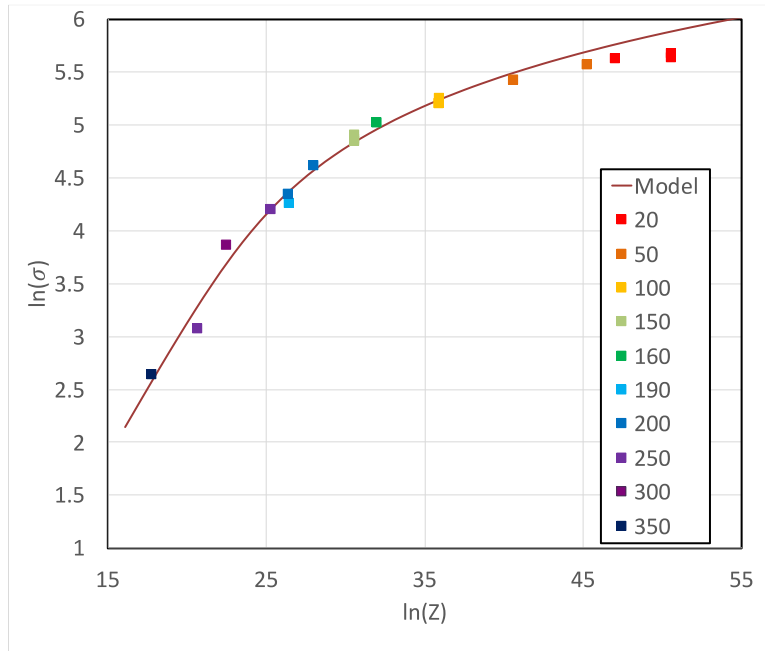
$$Z = A \{\sinh(\alpha\sigma)\}^n \quad \text{Eq 8}$$

At low stress (or  $Z$ ) conditions, this relationship asymptotes to a simple power law indicative of high temperature creep, whereas it asymptotes to an exponential function of stress at high stresses, which is typical of thermally activated slip. That is, it does a reasonably good job of describing both the power-law and power-law breakdown regimes. The empirical parameters  $A$ ,  $\alpha$ ,  $n$ , and  $Q$  were obtained by least-squares non-linear regression.

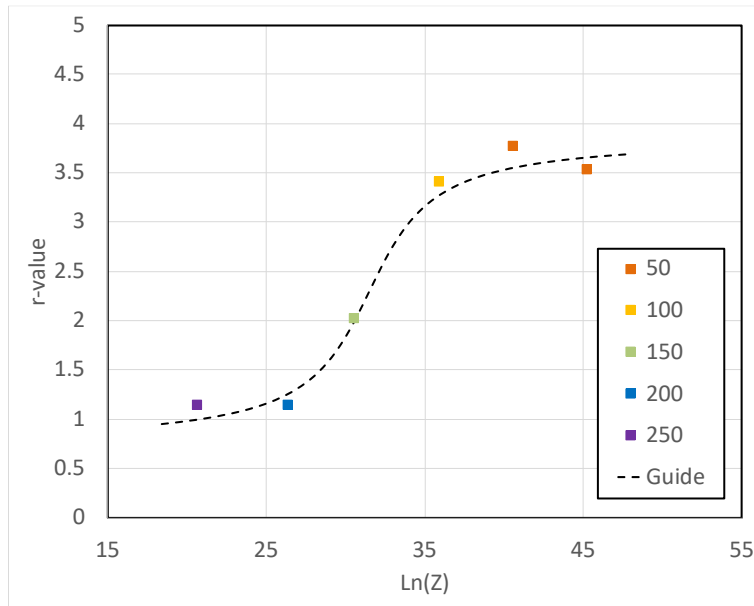
## Experimental results

Figure 1 presents the flow stress during uniaxial straining parallel to the TD, at a tensile plastic strain of 0.10, plotted as a function of the Zener-Holloman parameter,  $Z$ . Superimposed on the experimental data is a best-fit Sellars-Tegart function (Eq. 8), where the stress exponent  $n = 3.8$ . Such a value suggests that the rate-controlling deformation mechanism is dislocation climb at conditions of  $Z \sim 24$  or less. The transition to rate insensitive plasticity (or power-law breakdown) occurs over the range of  $24 \leq Z \leq 40$ . At higher  $Z$  levels, the plasticity is clearly rate-insensitive, and even the Sellars-Tegart function fails to describe the flow stress well. As such, the focus of this study is placed upon examining the texture evolution and strain anisotropy over these same three  $Z$ -value regimes (low, intermediate, high).

Figure 2 presents the  $r$ -value measured at a plastic tensile strain of 0.08 – 0.12 and plotted as a function of applied  $Z$ . As was observed above, there are three regimes, a low  $Z$  regime in which the  $r$ -value is close to 1 (near plastic isotropy), an intermediate regime, and a high  $Z$  regime in which the  $r$ -value is  $\sim 3.5$ . It is notable to the present authors that the transitions in  $r$ -value occur at nearly the same points that the constitutive relationship between flow stress and applied  $Z$  exhibit transitions. Specifically, under conditions where the constitutive modeling suggests the onset of significant strain accommodation by dislocation climb, the  $r$ -value begins to decrease.



**Figure 1.** Plot of log-stress vs. log-Z (where Z is the temperature-compensated strain rate or Zener-Holloman parameter, with a best-fit activation energy of ~140 kJ/mol.



**Figure 2.** The r-value (ratio of the width strain to the thickness strain) for samples of textured Mg alloy, AZ31B, sheet material tested parallel to the sheet transverse direction (TD) at the aforementioned temperatures and strain rates (see Figures 1). The dotted curve is merely to guide the eye, but suggests three mechanistic regimes at low, intermediate, and high Z values.

Finally, the crystallographic texture and its evolution after tensile deformation within each of the aforementioned Z-regimes is presented in Fig. 3. Note that a near 6-fold symmetry develops in the prismatic  $(10\bar{1}0)$  pole figures, within the high Z regime, which is indicative of significant activity of

the prismatic slip of  $\langle a \rangle$  dislocations. This significant non-basal slip of  $\langle a \rangle$  dislocations has been used to explain the observed high  $r$ -values of this basal textured sheet material [2]. As the temperature is increased (and  $Z$ -value is correspondingly decreased), the texture evolution undergoes a transition, whereby this characteristic 6-fold symmetry fades and then disappears. In the low  $Z$  regime, where the  $r$ -value approaches 1, the prismatic  $(10\bar{1}0)$  pole figure exhibits radial symmetry.

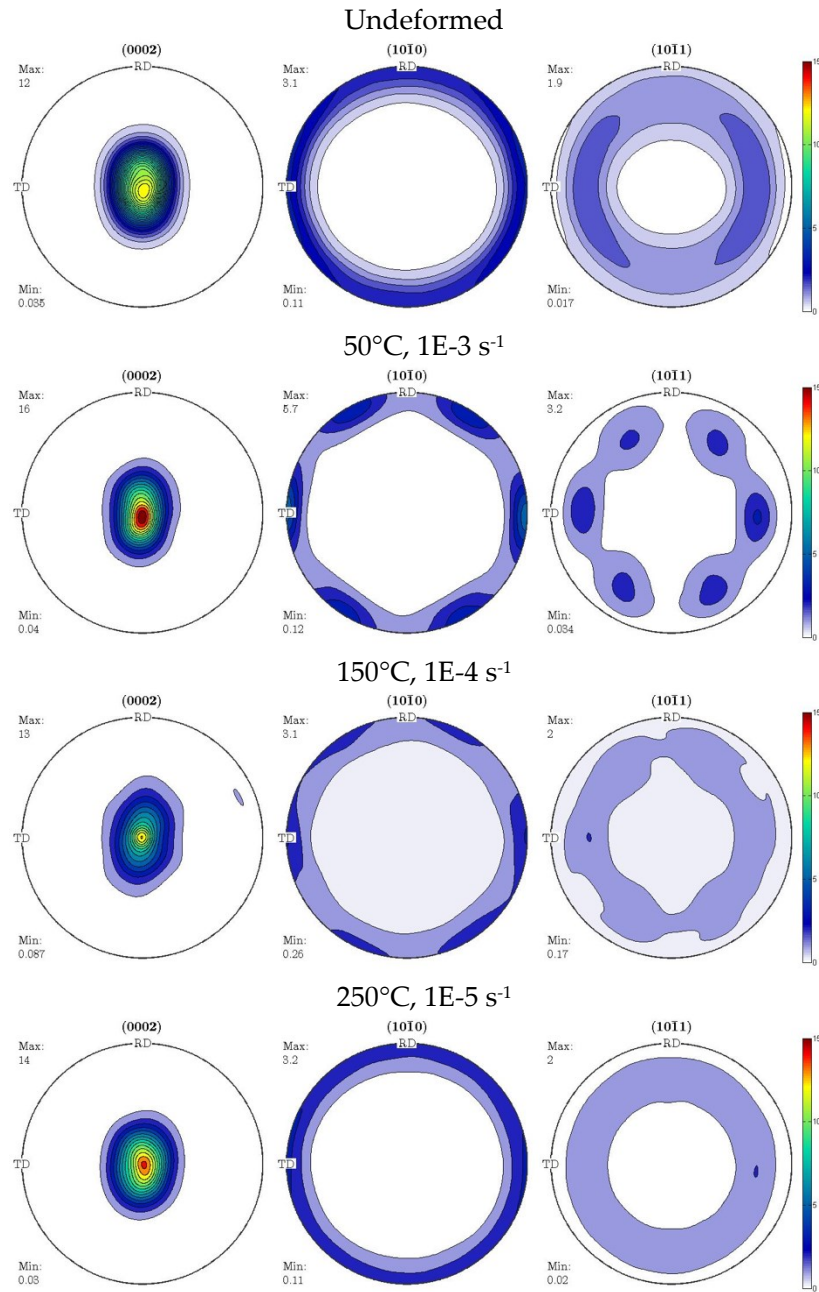


**Figure 3.** Crystallographic textures of samples of textured, commercial Mg alloy AZ31B sheet material tensile tested parallel to the sheet transverse direction (TD) at the conditions listed in the figure.



## Modeling results

Numerous authors have explored the effects of varying the critical resolved shear stress (CRSS) ratios of basal, prismatic  $\langle a \rangle$  and pyramidal  $\langle c+a \rangle$  slip can have on the  $r$ -values and texture evolutions [e.g., 20]. Here we present a succinct review of those effects and add to it the effect of climb of basal  $\langle a \rangle$  type dislocations. For the present basal texture, the predicted  $r$ -values after simulations up to a plastic strain of 0.20 are presented in Fig. 4. The region colored aqua includes  $r$ -values typical of the present study at high  $Z$  (low temperature). The regime where the ratio between strength of  $\langle c+a \rangle$  and prismatic slip  $\sim 1$  is where the  $r$ -values approach 1. The portion of the figure where  $\langle c+a \rangle$  is much softer than prismatic slip is viewed as unfeasible (and colored black).

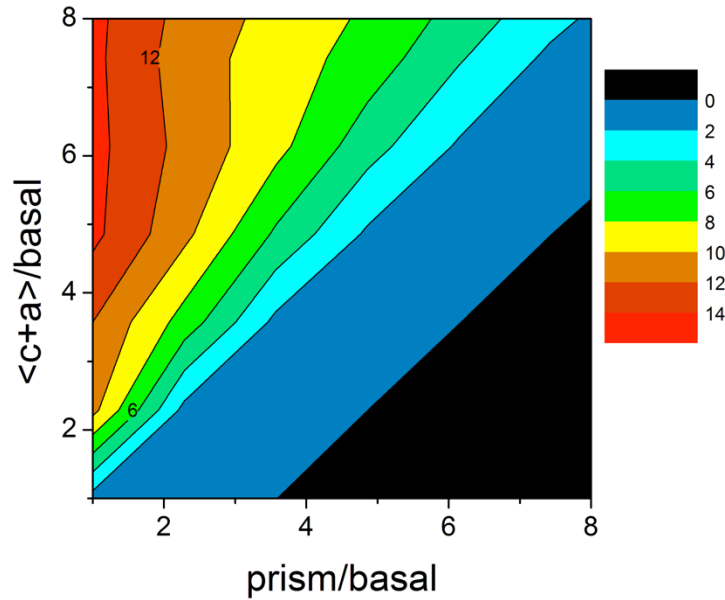


**Figure 4.**  $r$ -values plotted as a function of CRSS ratios ranging from 1 to 8 for slip of  $\langle c+a \rangle$  and prismatic  $\langle a \rangle$  dislocations.

The simulated textures after a TD tensile strain of 0.20 are presented in Fig. 5. The first texture is typical of the high  $Z$  regime, where prismatic slip is quite active and the  $r$ -value is high. The second texture is typical of what happens if the CRSS for  $\langle c+a \rangle$  slip is reduced sufficiently to induce an  $r$ -value near 1. Notably, the 6-fold symmetry in the prismatic pole figure remains, and in some cases (only slight in the present case), the basal pole figure exhibits splitting toward the TD. Finally, a case is shown in which the predicted  $r = 1.2$  and the predicted prismatic pole figure exhibits radial symmetry, both of which are features that match what is observed experimentally (see Figs. 2 & 3). Surprisingly, despite having a higher critical (normal) stress for climb, as compared to the CRSS values for glide on any slip system, climb was shown to accommodate 80% of the strain in this example where the  $r$ -value and texture evolution match that observed experimentally. Only when the activity of prismatic  $\langle a \rangle$  slip is reduced to a low level (nil), is the appearance of the 6-fold symmetry in the  $(10\bar{1}0)$  pole figures eliminated.

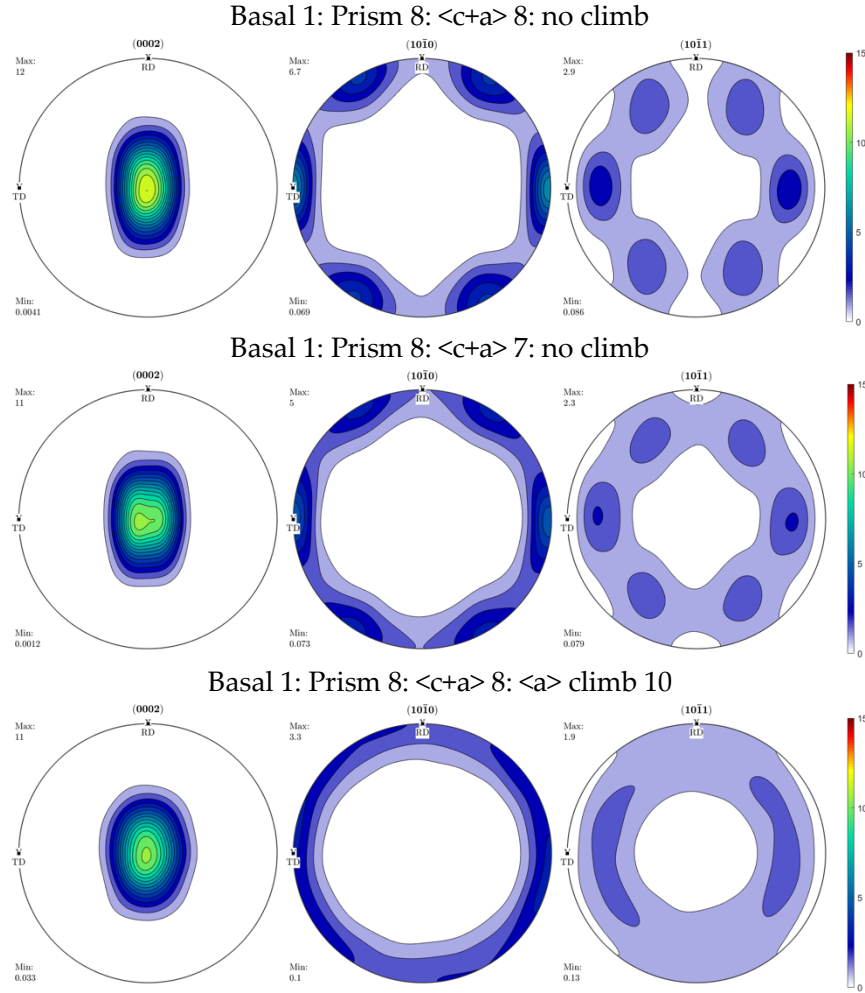


**Figure 5.** Predicted textures which evolve for model cases in which the  $r$ -values match the high  $Z$  (low temperature) regime and those which match the low  $Z$  regime by increasing the activity of  $\langle c+a \rangle$  slip or basal  $\langle a \rangle$  dislocation climb. The numbers in the figure headings indicated the relative CRSS and critical climb stress values employed in the simulations. Intermediate cases (in terms of  $r$ -value and texture) are obtained by incorporating an intermediate level of dislocation climb.

## Discussion

Dislocation climb and cross-glide are obviously relevant to applications involving creep, load relaxation (such as bolt-load retention), and hot/warm forming operations. However, there are vast fundamental unknowns, since much of the current thinking about the warm deformation of Mg is dominated by considerations of which dislocation glide mechanisms are operative, deformation twinning and grain boundary sliding [21,22], despite the fact that the measured constitutive response of Mg and its alloys frequently exhibits power-law type constitutive behavior [e.g., 23]. Rarely have crystal plasticity modelers considered these aspects, though the work of Staroselsky and Anand [24], notably considered the possible role of grain boundary sliding. Here, it has been hypothesized that the behavior of Mg alloys (flow strength, ductility, formability, etc.) could be as much controlled by thermally activated motion of dislocations out of their glide planes as it is by glide motion.

It is further noted that the interplay between cross-slip and climb is subject to controversy. Historically, there has been significant opposition to the notion of cross-slip controlled creep [25]. In



fact, a recent monograph on creep suggests that though the issue has not reached consensus, “it is widely accepted that the activation energy for [power law] creep closely corresponds to that of lattice self-diffusion.” [26] However, Poirier [27] advances the very reasonable notion that cross-slip of screw dislocations and climb of edge (and mixed) dislocations are mechanisms that must occur in parallel. There have been strong arguments, based upon experimental evidence, that Mg [28], Mg-Al [29], and very recently, a Zr alloy [30] undergo cross-slip controlled creep. On the other hand, while it is accepted that cross-slip of  $\langle a \rangle$  dislocations from the basal plane onto the prismatic plane may be the rate controlling mechanism at some temperatures, Couret & Caillard [31] assert that cross-glide cannot be controlling at the highest temperatures, as previously claimed [e.g., 32,33], because their in-situ TEM results show cross-glide to be very easy at those temperatures. Instead, they hypothesize cross-slip control at intermediate temperatures and  $[c]$  dislocation climb-control at the highest temperatures.

Indeed, there are a large number of thermally activated deformation mechanisms which can be rate controlling, in the case of hexagonal close-packed Mg and its alloys, depending upon (at least): temperature, applied stress level (or strain rate), and the state of stress. These mechanisms include: climb of basal  $\langle a \rangle$  and non-basal  $[c]$  dislocations; glide of the harder, non-basal dislocations (e.g., pyramidal glide of  $\langle c+a \rangle$  dislocations); grain boundary sliding; and diffusional flow. The higher stress conditions presently of interest ensure that diffusional flow will not be controlling. However, the other mechanisms are real candidates. Curiously, dislocations with  $[c]$  Burgers vectors have been discussed far less in the recent literature. One reason is the fact that there is no loading condition that will favor the glide of these large Burgers vector dislocations over  $\langle a \rangle$  type dislocations. However, past investigations of Edelin and Poirier [34] found climb of basal dislocation loops with  $[c]$  Burgers vectors to be the controlling mechanism, during  $c$ -axis compression of single crystals, rather than glide of  $\langle c+a \rangle$  dislocations. These ideas undergird the present hypothesis that *climb may sometimes obviate the need for hard dislocation slip*.

## Conclusions

Measurements of the flow stress,  $r$ -values, and texture evolution during TD tension of basal textured Mg alloy AZ31B sheets have revealed three behavioral regimes corresponding to low ( $Z < 24$ ), intermediate ( $24 \leq Z \leq 40$ ), and high ( $Z > 40$ ) rate regimes. Simple constitutive modeling reveals the behavior within each of these regimes to be characteristic of power-law creep, power-law breakdown, and thermally activated plasticity, respectively. Within the high  $Z$ , thermally activated plasticity regime, non-basal slip of  $\langle a \rangle$  dislocations is shown to prevail and explains the widely observed high  $r$ -values and the 6-fold symmetry which develops within the  $(10\bar{1}0)$  pole figures. A new crystal plasticity model, which incorporates the strain and reorientation characteristic of dislocation climb is used to show that the transitions in both the  $r$ -value and texture evolution can be described if one accounts for dislocation climb of basal  $\langle a \rangle$  dislocations. The present report only scratches the surface and numerous areas remain to be explored, such as the possible roles of other climb modes and the possible effects distinct rate sensitivities of the various climb and glide modes.

## Acknowledgements

The authors would like to thank the United States National Science Foundation, Division of Materials Research, Metals and Metallic Nanostructures (NSF-DMR- MMN) program, Grant No. 1810197, overseen by program manager Dr. Lynnette Madsen, for financial support of this research.

## References

---

1. C.S. Roberts, "The Deformation of Magnesium", in *Magnesium and Its Alloys*, (New York: John Wiley, 1960), p. 81–107.
2. Agnew, S. R. (2002). Plastic anisotropy of magnesium alloy AZ 31 B sheet. In *Magnesium Technology 2002 as held at the 2002 TMS Annual Meeting* (pp. 169-174).
3. Agnew, S. R., & Duygulu, Ö. (2005). Plastic anisotropy and the role of non-basal slip in magnesium alloy AZ31B. *International Journal of plasticity*, 21(6), 1161-1193.
4. Sandlöbes, S., Zaefferer, S., Schestakow, I., Yi, S., & Gonzalez-Martinez, R. (2011). On the role of non-basal deformation mechanisms for the ductility of Mg and Mg–Y alloys. *Acta Materialia*, 59(2), 429-439.
5. Sandlöbes, S., Pei, Z., Friák, M., Zhu, L. F., Wang, F., Zaefferer, S., ... & Neugebauer, J. (2014). Ductility improvement of Mg alloys by solid solution: Ab initio modeling, synthesis and mechanical properties. *Acta Materialia*, 70, 92-104.
6. Fan, H., & El-Awady, J. A. (2015). Towards resolving the anonymity of pyramidal slip in magnesium. *Materials Science and Engineering: A*, 644, 318-324.
7. Wu, Z., & Curtin, W. A. (2015). The origins of high hardening and low ductility in magnesium. *Nature*, 526(7571), 62.
8. Wu, Z., & Curtin, W. A. (2016). Mechanism and energetics of  $\langle c+a \rangle$  dislocation cross-slip in hcp metals. *Proceedings of the National Academy of Sciences*, 113(40), 11137-11142.
9. Wu, Z., Ahmad, R., Yin, B., Sandlöbes, S., & Curtin, W. A. (2018). Mechanistic origin and prediction of enhanced ductility in magnesium alloys. *Science*, 359(6374), 447-452.
10. Lebensohn, R. A., Hartley, C. S., Tomé, C. N., & Castelnau, O. (2010). Modeling the mechanical response of polycrystals deforming by climb and glide. *Philosophical Magazine*, 90(5), 567-583.
11. Lebensohn, R. A., Holt, R. A., Caro, A., Alankar, A., & Tomé, C. N. (2012). Improved constitutive description of single crystal viscoplastic deformation by dislocation climb. *Comptes Rendus Mecanique*, 340(4), 289-295.
12. Izadbakhsh, A., Inal, K., Mishra, R. K., & Niewczas, M. (2011). New crystal plasticity constitutive model for large strain deformation in single crystals of magnesium. *Computational materials science*, 50(7), 2185-2202.
13. Proust, G., Tomé, C. N., Jain, A., & Agnew, S. R. (2009). Modeling the effect of twinning and detwinning during strain-path changes of magnesium alloy AZ31. *International Journal of Plasticity*, 25(5), 861-880.
14. Kocks, U. F., Tomé, C. N., & Wenk, H. R. (2000). *Texture and anisotropy: preferred orientations in polycrystals and their effect on materials properties*. Cambridge university press.
15. Arsenlis, A., & Parks, D. M. (1999). Crystallographic aspects of geometrically-necessary and statistically-stored dislocation density. *Acta Materialia*, 47(5), 1597-1611.
16. Lebensohn, R. A., Holt, R. A., Caro, A., Alankar, A., & Tomé, C. N. (2012). Improved constitutive description of single crystal viscoplastic deformation by dislocation climb. *Comptes Rendus Mecanique*, 340(4), 289-295.
17. Polesak, F., Dreyer, C., Shultz, T., & Agnew, S. (2009). Blind study of the effect of processing history on the constitutive behaviour of alloy AZ31B. *Magnesium Technology 2009*, 491-496.

- 
18. ASTM E 2448 – 06, “Standard Test Method for Determining the Superplastic Properties of Metallic Sheet Materials” (ASTM International, West Conshohocken, PA, 2006).
  19. C.M. Sellars, W.J. Tegart, “Relationship between strength and struture in deformation at elevated temperature,” *Mem. Sci. Rev. Metall.*, 63 (1967) 731-745.
  20. Miller, V. M., Berman, T. D., Beyerlein, I. J., Jones, J. W., & Pollock, T. M. (2016). Prediction of the plastic anisotropy of magnesium alloys with synthetic textures and implications for the effect of texture on formability. *Materials Science and Engineering: A*, 675, 345-360.
  21. Luo, A. A., Powell, B. R., & Balogh, M. P. (2002). Creep and microstructure of magnesium-aluminum-calcium based alloys. *Metallurgical and Materials Transactions A*, 33(3), 567-574.
  22. Koike, J., Ohyama, R., Kobayashi, T., Suzuki, M., & Maruyama, K. (2003). Grain-boundary sliding in AZ31 magnesium alloys at room temperature to 523 K. *Materials Transactions*, 44(4), 445-451.
  23. Somekawa, H., Hirai, K., Watanabe, H., Takigawa, Y., & Higashi, K. (2005). Dislocation creep behavior in Mg–Al–Zn alloys. *Materials Science and Engineering: A*, 407(1), 53-61.
  24. Staroselsky, A., & Anand, L. (2003). A constitutive model for hcp materials deforming by slip and twinning: application to magnesium alloy AZ31B. *International journal of Plasticity*, 19(10), 1843-1864.
  25. Sherby, O. D., & Weertman, J. (1979). Diffusion-controlled dislocation creep: a defense. *Acta Metallurgica*, 27(3), 387-400.
  26. Kassner, M. E. (2015). *Fundamentals of creep in metals and alloys*. Butterworth-Heinemann.
  27. Poirier, J.-P. (1985) Power-law creep and self-diffusion, in *Creep of crystals: High-temperature deformation processes in metals, ceramics, and minerals*, Cambridge University Press, pp. 111-114.
  28. Vagarali, S. S., & Langdon, T. G. (1981). Deformation mechanisms in hcp metals at elevated temperatures—I. Creep behavior of magnesium. *Acta Metallurgica*, 29(12), 1969-1982.
  29. Vagarali, S. S., & Langdon, T. G. (1982). Deformation mechanisms in hcp metals at elevated temperatures—II. Creep behavior of a Mg-0.8% Al solid solution alloy. *Acta Metallurgica*, 30(6), 1157-1170.
  30. Kombaiah, B., & Murty, K. L. (2015). Dislocation cross-slip controlled creep in Zircaloy-4 at high stresses. *Materials Science and Engineering: A*, 623, 114-123.
  31. Couret, A., & Caillard, D. (1985). An in situ study of prismatic glide in magnesium—I. The rate controlling mechanism. *Acta Metallurgica*, 33(8), 1447-1454.
  32. Vagarali, S. S., & Langdon, T. G. (1981). Deformation mechanisms in hcp metals at elevated temperatures—I. Creep behavior of magnesium. *Acta Metallurgica*, 29(12), 1969-1982.
  33. Vagarali, S. S., & Langdon, T. G. (1982). Deformation mechanisms in hcp metals at elevated temperatures—II. Creep behavior of a Mg-0.8% Al solid solution alloy. *Acta Metallurgica*, 30(6), 1157-1170.
  34. Edelin, G., & Poirier, J. P. (1973). Etude de la montée des dislocations au moyen d'expériences de fluage par diffusion dans le magnésium: II. Mesure de la vitesse de montée. *Philosophical Magazine*, 28(6), 1211-1223.